Nonlinear Dynamics and Chaos

Prof. George Haller
Transcription: Trevor Winstral

2022

Contents

Chapter 1

Introduction

First we shall introduce the most important characters in our following exploration. The ideas and definitions here will be recurring regularly as we examine them from different perspectives and using different tools. The content covered by this course can be found in the following books. For further details on some of the results, we recommend consulting these.

- J. Guckenheimer & P. Holmes, Nonlinear Oscillations, Dynamical Systems and Bifurcations of Vector Fields,

- F. Verhulst, Nonlinear Differential Equations and Dynamical Systems,

- V. I. Arnold, Ordinary Differential Equations,

- S. Strogatz, Nonlinear Dynamics and Chaos.

Definition 1.1 (Dynamical System (DS)). A triple $(P, E, \mathcal{F})$, with

- P : the phase space for the dynamical variable $\mathbf{x} \in P$,

- E : base space of the evolutionary variable (e.g. time) $t \in E$,

- $\mathcal{F}$: the evolution rule (deterministic) which defines the transition from one state to the next.

The two main types of evolutionary variable spaces are

(i) Discrete dynamical systems (DDS) $t \in E = \mathbb{Z}$ with trajectory $\{\mathbf{x}_0, \mathbf{x}_1, \ldots\}$,

(ii) Continuous dynamical systems (CDS) $t \in E = \mathbb{R}$ with trajectory $\{\mathbf{x}_t\}_{t \in \mathbb{R}}$.

Corresponding to these there are various types of evolution rules

(i) In a DDS we have iterated mappings

$$\mathbf{x}_{n+1} = F(\mathbf{x}_n, n).$$

If there is no explicit dependence on n, i.e. $\frac{\partial F}{\partial n} = 0$, then

$$\mathbf{x}_{n+1}F(\mathbf{x}_n) = F(F(\mathbf{x}_{n-1})) = \underbrace{F \circ \ldots \circ F}_{n+1 \text{ times}}(\mathbf{x}_0) = F^{n+1}(\mathbf{x}_0).$$

Example 1.1 (Cobweb diagram of a one-dimensional DDSs). In such cases and in one-dimensional problems, a simple way to analyze the behavior of the system is the so-called *cobweb* diagram. We may plot x_{n+1} as a function of x_n, as demonstrated in Fig. 1.1. The image of an initial condition x_0 lies on the graph at $x_{n+1} = F(x_0)$. We can also compute the next iterate by horizontally projecting the point $(x_0, F(x_0))$ to the diagonal line defined by $x_{n+1} = x_n$. Following the porjection of this point to the horizontal axis (x_n) we find the intersection with the graph at the point $(x_1, F(x_1))$. It follows that fixed points on the cobweb diagram, correspond to the intersection of the graph of F with the diagonal line $x_{n+1} = x_n$.
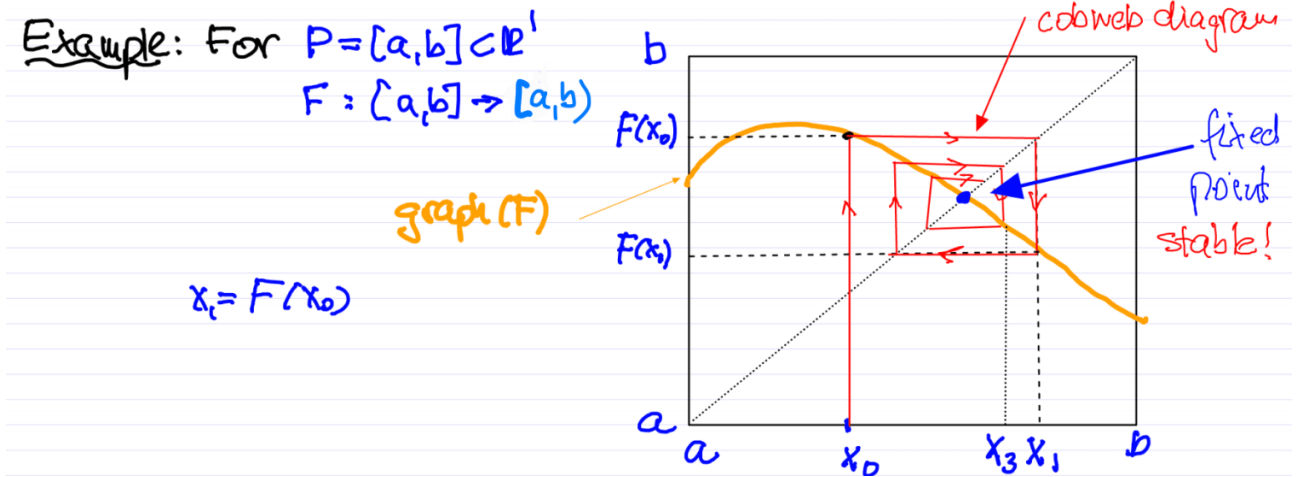

Figure 1.1: Analysis of a one-dimensional system defined on the interval $x \in [a, b]$ using the cobweb diagram

(ii) In a CDS we have a first order system of ordinary differential equations (ODE)

$$\dot{\mathbf{x}} = f(\mathbf{x}, t)$$

for $\mathbf{x} \in P$ and $t \in E$. This yields the initial value problem (IVP):

$$\begin{cases} \dot{\mathbf{x}} = f(\mathbf{x}, t) \\ \mathbf{x}(t_0) = \mathbf{x}_0 \end{cases}$$

Assuming there exists a unique solution $\varphi(t; t_0, \mathbf{x}_0)$ with $\dot{\varphi} = f(\phi, t)$ and $\varphi(t_0) = \mathbf{x}_0$, then the following flow map is well defined

$$\boxed{F_{t_0}^t(\mathbf{x}_0) := \varphi(t; t_0, \mathbf{x}_0).}$$

Geometrically, this solution can be viewed as a trajectory in phase space (cf. Fig. 1.2).
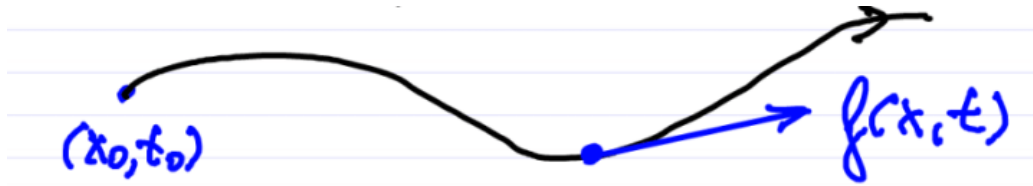

Figure 1.2: Trajectory of a continuous dynamical system. The RHS is given by f(x,t), which is the tangent vector to this curve at the point x at time t.

Such an $F_{t_0}^t$ has the properties

(a) $F_{t_0}^t$ is as smooth as $f(\mathbf{x}, t)$,

(b) $F_{t_0}^{t_0} = I$ and $F_{t_0}^{t_2} = F_{t_1}^{t_2} \circ F_{t_0}^{t_1}$,

(c) $\left(F_{t_0}^t\right)^{-1} = F_t^{t_0}$ exists and is smooth.

Properties (ii) and (iii) together are called the group property. A special case of continuous dynamical systems is the autonomous system.

$$\boxed{\dot{\mathbf{x}} = f(\mathbf{x}).}$$

The autonomy of a system implies

$$\mathbf{x}(s, t_0, \mathbf{x}_0) = \mathbf{x}(\underbrace{s - t_0}_{t}, 0, \mathbf{x}_0) \overset{!}{=} \mathbf{x}(t, \mathbf{x}_0).$$

The induced flow map in this case is the one-parameter family of maps

$$\boxed{F^t = F_0^t : \mathbf{x}_0 \mapsto \mathbf{x}(t, \mathbf{x}_0).}$$

Example 1.2 (Logisitic Equation). For a resource-limited population, we have the following dynamical system for $a > 0$, $b > 0$, and the population $x \in \mathbb{R}_+ \cup \{0\}$

$$\dot{x} = ax(b - x).$$

In this case we have $E = \mathbb{R}$ and $\mathcal{F} = \{F^t\}_{t=-\infty}^{+\infty}$. This system has globally existing unique solutions (see later). We may analyze the behavior of this system by plotting $\dot{x}$ as a function of x, analogously to the cobweb diagram. This is demonstrated in Fig. 1.3. At x values, where $\dot{x}$ is positive $x(t)$ is growing, while at negative values it is decreasing. This means, that fixed points, at which $x(t) = \text{const.}$ correspond to intersections of the graphs with the horizontal axis.
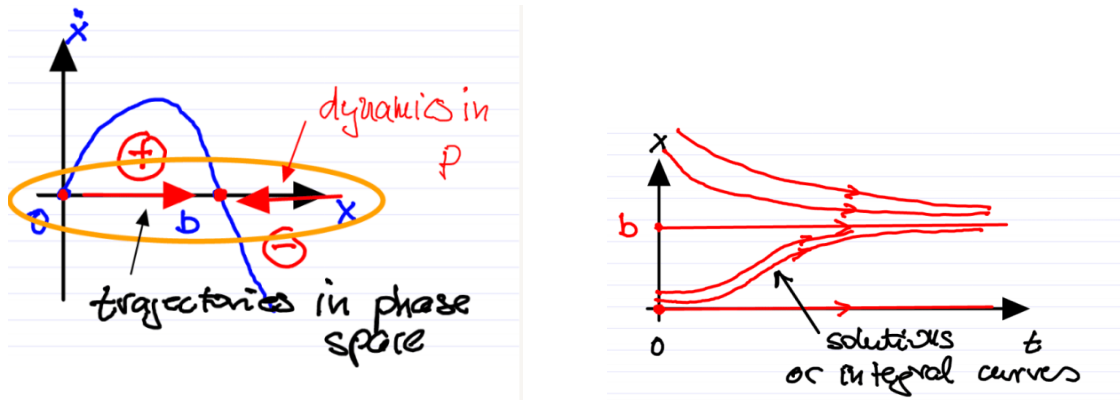

Figure 1.3: Left: Analysis of the right hand side. Right: Evolution in the extended phase space $P \times \mathbb{R}$.

Example 1.3 (Pendulum). Given the equation of motion

$$ml^2\ddot{\varphi} = -mgl\sin(\varphi).$$

We let $x_1 = \varphi$ and $\mathbf{x}_2 = \dot{\varphi}$ to transform into the first-order ODE form

$$\begin{cases} \dot{x}_1 = x_2 \\ \dot{x}_2 = -\dfrac{g}{l}\sin(x_1). \end{cases}$$

Thus we have

$$\mathbf{x} = \begin{pmatrix} x_1 \\ x_2 \end{pmatrix}; \quad f(\mathbf{x}) = \begin{pmatrix} x_2 \\ -\frac{g}{l}\sin(x_1) \end{pmatrix}.$$

Qualitative analysis gives the following facts

- $(x_1, x_2) = (0, 0)$ and $(x_1, x_2) = (\pi, 0)$ are zeros of f.

- Energy is conserved, hence both small and large amplitude oscillations are expected.

- The function $f(x)$ has symmetries: it is invariant under the transformation $(x_1, x_2, t) \mapsto (x_1, -x_2, -t)$ and $(x_1, x_2, t) \mapsto (-x_1, x_2, -t)$. See the left panel of Fig. 1.4.
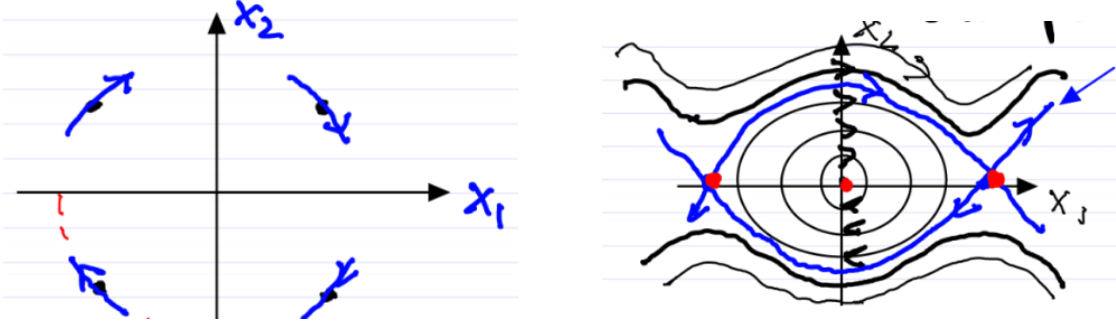

Figure 1.4: Left: The symmetries of the dynamical system. Right: Phase portrait of the pendulum. Red dots show the fixed points, while the blue trajectories make up the separatrix.

Definition 1.2. A separatrix is a boundary (i.e. a codimension-1 surface) in phase space which separates regions of qualitatively different behaviors. In practice, it is unobservable by itself and connects different fixed points. The separatrix of the pendulum is shown in the right panel of Fig. 4.

Example 1.4 (Exploit geometry of phase space for analysis). Consider two cities, A and B. The two cities are connected by two roads, denoted by the blue and green curves of the left panel of Fig. 1.5. We assume that travelling on the two roads, it is possible for two bikes to make it from A to B without ever being further away from each other than a distance $d < D$.

Assume two trucks are trying to make it between A and B, on different roads in the opposite direction, carrying a load of width D. Given this information, can the trucks make it without hitting each other? We can view this problem as a continuous dynamical system with two coordinates x_1 and x_2 that parameterize the two routes between A and B. This dynamical system is, in general, non autonomous.

The right panel of Fig 1.5 shows the trajectories of the two trucks and the two bikes in phase space. The two trajectories must intersect by continuity, thus at that point the trucks must be at the same positions as the bikes, implying they are within distance D. Therefore the trucks must crash!
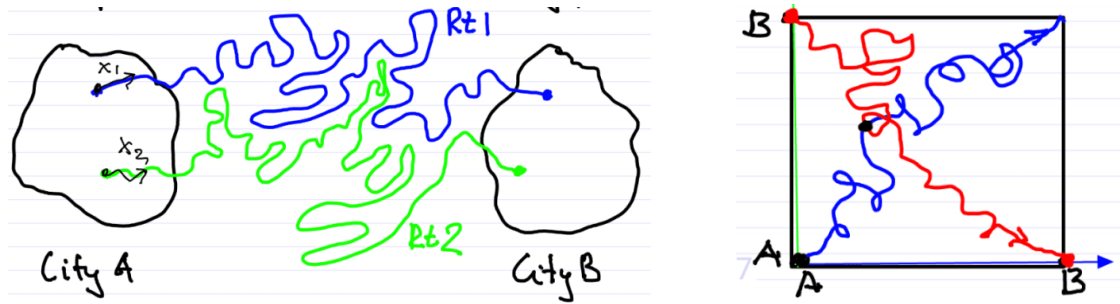
Figure 1.5: Left: An example of the two bike routes. Right: Blue represents the trajectory of the two bikes, red represents the trajectory of the two trucks.

Chapter 2

Fundamentals

In this chapter, we first review some fundamental properties of continuous dynamical systems that will be used heavily in later chapters. As we will see, these technical results are interesting in their own right. They can help in interpreting or cross-checking numerical results or physical models for self-consistency or accuracy.

2.1 Existence and uniqueness of solutions

Consider

$$\begin{cases} \dot{\mathbf{x}} = f(\mathbf{x}, t); & \mathbf{x} \in \mathbb{R}^n \\ \mathbf{x}(t_0) = \mathbf{x}_0 \end{cases}.$$

Does this initial value problem have a unique solution? We have the following theorems to help us answer that question.

Theorem 2.1 (Peano). *If $f \in C^0$ near $(\boldsymbol{x}_0, t_0)$, then there exists a local solution $\varphi(t)$, i.e.,*

$$\dot{\varphi}(t) = f(\varphi(t), t), \varphi(t_0) = x_0; \ \forall t \in (t_0 - \epsilon, t_0 + \epsilon); \ 0 < \epsilon \ll 1.$$

Example 2.1 (Free falling mass). Consider a point mass of mass m at position x. The acceleration due to gravity is denoted by g. Measuring the potential energy from the reference point $x = x_0$, we have the total energy is conserved.

$$\frac{1}{2} m \dot{x}^2 = mg(x - x_0).$$

This implies that

$$\begin{cases} \dot{x} = \sqrt{2g(x - x_0)} \\ x(0) = x_0 \end{cases}$$

on the set $P = \{x \in \mathbb{R} : x \geq x_0\}$. Therefore we have that $f \in C^0$ in phase space, so by Peano's theorem (cf. Theorem 2.1), there exists a local solution. A schematic diagram is shown in Fig. 2.1. The solution is actually $x(t) = x_0 + \frac{g}{2}(t - t_0)^2$, however $x(t) = x_0$ is also a solution to
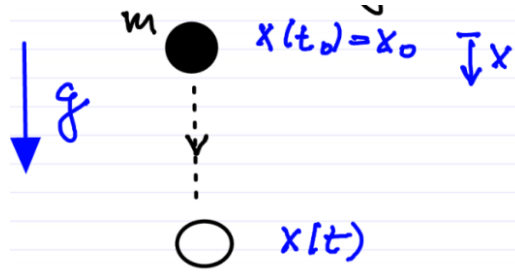

Figure 2.1: Schematic diagram of the point mass in free fall.

the IVP, therefore we do not have a unique solution. Physically there exists a solution, but this IVP was derived from a heuristic energy-principle, not from Newton's laws, which are not equivalent.

Definition 2.1. A function f is called locally Lipschitz around $\mathbf{x}_0$ if there exists an open set $U_{\mathbf{x}_0}$ and $L > 0$ such that for all $\mathbf{x}, \mathbf{y} \in U_{\mathbf{x}_0}$

$$\|f(\mathbf{y}, t) - f(\mathbf{x}, t)\| \leq L\|\mathbf{y} - \mathbf{x}\|.$$

Example 2.2 (Lipschitz functions). Fig. 2.2 shows an example of a Lipschitz and a non-Lipschitz function around x_0.
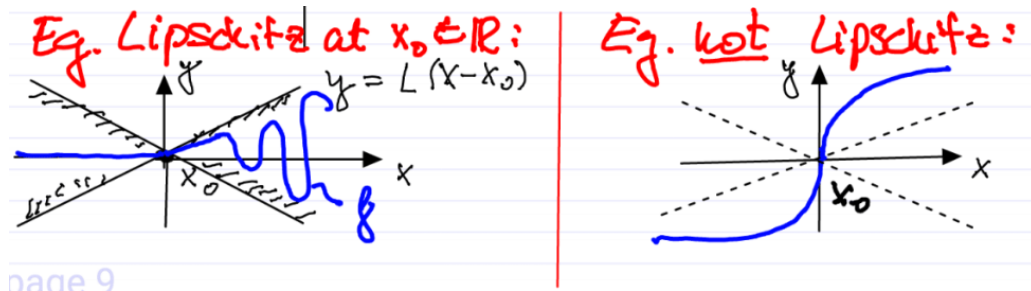

Figure 2.2: Interpretation of the Lipschitz property.

Theorem 2.2 (Picard). *Assume*

   (i) $f \in C^0$ *in t near $(t_0, \boldsymbol{x}_0)$,*

   (ii) f *is locally Lipschitz in $\boldsymbol{x}$ near $(t_0, \boldsymbol{x}_0)$.*

Then there exists a unique local solution to the IVP. The proof can be found in Arnold's book on ODEs.

Note the following relations. If f is $C^1 \implies f$ is Lipschitz $\implies f$ is C^0.

Example 2.3 (Free falling mass revisted). We check if f is Lipschitz.

$$\frac{\|f(x) - f(x_0)\|}{\|x - x_0\|} = \frac{\sqrt{2g}}{\sqrt{\|x - x_0\|}} \geq L\|x - x_0\|.$$

Thus f is not Lipschitz near x_0.

2.2   Geometric consequences of uniqueness

If the solution is unique, we have a few facts that can be derived from the geometric point of view.

(i) The trajectories of autonomous systems cannot intersect. Note that fixed points do not violate this (e.g. pendulum equations). See Fig. 2.3 which shows the phase portrait of the pendulum.
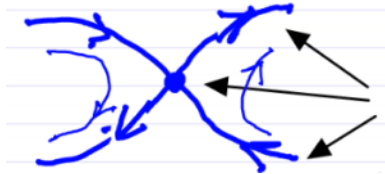

Figure 2.3: The phase portrait of the pendulum. Trajectories do not intersect since each arrow is pointing at separate trajectories.

(ii) For non-autonomous systems, intersections in phase space are possible: a trajectory may occupy the same point x at a different time instants (see the left panel of Fig. 2.4. In this case we can extend the phase space in order to get an autonomous system where there cannot be any intersections.

$$\mathbf{X} = \begin{pmatrix} \mathbf{x} \\ t \end{pmatrix}, \ F(\mathbf{X}) = \begin{pmatrix} f(\mathbf{x}, t) \\ 1 \end{pmatrix}; \ \dot{\mathbf{X}} = F(\mathbf{X}).$$
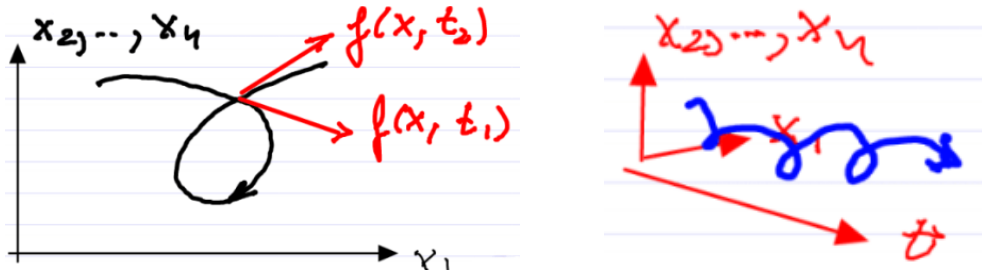
Figure 2.4: Left: Intersecting trajectories in phase space for a non-autonomous system. Right: The same trajectory in the extended phase space, without intersections.

2.3   Local vs global existence

Example 2.4 (Exploding solution).

$$\begin{cases} \dot{x} = x^2 \\ x(t_0) = 1. \end{cases}$$

Integrating yields the solution $x(t) = \frac{1}{1-(t-t_0)}$. This solution blows up at $t_\infty = t_0 + 1$, therefore the solution is only local. This is demonstrated in Fig. 2.5.
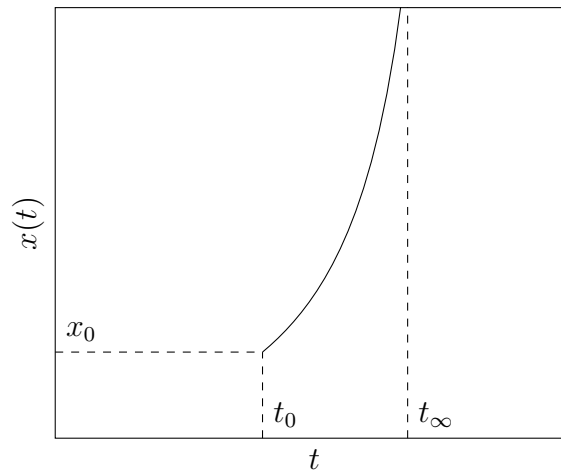

Figure 2.5: Solution to the ODE $\dot{x} = x^2$ started from $x(t_0) = 1$.

To address this problem of local solutions not being able to be continued into global solution, we have the following theorem.

Theorem 2.3 (Continuation of solution)**.** *If a local solutions cannot be continued to a time $t = T$, then we must have*

$$\boxed{\lim_{t \to T} \|\boldsymbol{x}(t)\| = \infty.}$$

The proof can be found in Arnold's book on ODEs.

Example 2.5 (Coupled Pendulum System). Consider two pendula of masses m_1 and m_2. They both have length l. The angles of these pendula are denoted by φ_1 and φ_2. Let us assume that they are coupled by a nonlinear spring, which can be described by a potential $V(\varphi_1, \varphi_2)$. This setup is illustrated in Fig. 2.6. We set $x_1 = \varphi_1$, $x_2 = \dot{\varphi}_1$, $x_3 = \varphi_2$, $x_4 = \dot{\varphi}_2$ and get the following equation of motion

$$\begin{cases} \dot{x}_1 = x_2 \\ \dot{x}_2 = \dots \\ \dot{x}_3 = x_4 \\ \dot{x}_4 = \dots \end{cases}$$

The RHS is smooth, therefore there exists a unique local solution to any IVP. The phase space
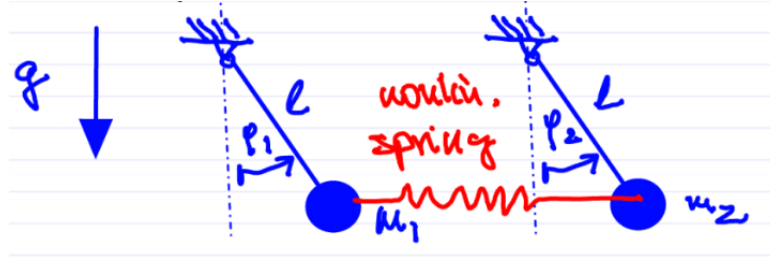

Figure 2.6: Physical setup of the coupled pendulum with a nonlinear spring.

is given by

$$P = \{\mathbf{x} : \ x_1 \in S^1, \ x_2 \in \mathbb{R}, \ x_3 \in S^1, \ x_4 \in \mathbb{R}\} = S^1 \times \mathbb{R} \times S^1 \times \mathbb{R}.$$

Where S^1 is the 1 dimensional sphere (i.e. a circle). With this space we know that $\|x_1\|$ and $\|x_3\|$ are bounded. Due to energy being conserved we have

$$E = T + V = \frac{1}{2} m_1 l_1 x_2^2 + \frac{1}{2} m_2 l_2 x_4^2 + \underbrace{V(x_1, x_3)}_{\geq 0}$$

$$E = E_0 = \text{constant} \geq 0.$$

Hence $\|x_2\|$ and $\|x_4\|$ are also bounded, therefore all solutions exist globally.

Definition 2.2. A linear system is one such that for $\mathbf{x} \in \mathbb{R}^n$, $\boldsymbol{A}(t) \in \mathbb{R}^{n \times n}$ and $\boldsymbol{A} \in C^0$

$$\dot{\mathbf{x}} = \boldsymbol{A}(t)\mathbf{x}.$$

Remark 2.4. Note that $\boldsymbol{A}$ can be written as $\boldsymbol{A} = \boldsymbol{S} + \boldsymbol{\Omega}$ where $\boldsymbol{S} = \frac{1}{2}(\boldsymbol{A} + \boldsymbol{A}^T)$ is symmetric (i.e. $\boldsymbol{S} = \boldsymbol{S}^T$) and $\boldsymbol{\Omega} = \frac{1}{2}(\boldsymbol{A} - \boldsymbol{A}^T)$ is skew symmetric (i.e. $\boldsymbol{\Omega} = -\boldsymbol{\Omega}^T$). Furthermore the eigenvalues of $\boldsymbol{S}$, λ_i, are all real and their respective eigenvectors, e_i, are orthogonal.

Example 2.6 (Global existence in linear systems).

$$\langle \mathbf{x}, \dot{\mathbf{x}} \rangle = \frac{1}{2} \frac{d}{dt} \|\mathbf{x}(t)\|^2 = \langle \mathbf{x}, \boldsymbol{A}(t)\mathbf{x} \rangle = \langle \mathbf{x}, (\boldsymbol{S}(t) + \boldsymbol{\Omega}(t))\mathbf{x} \rangle$$

$$= \langle \mathbf{x}, S(t)\mathbf{x} \rangle + \underbrace{\langle \mathbf{x}, \boldsymbol{\Omega}(t)\mathbf{x} \rangle}_{=0} \overset{(*)}{=} \sum_{i=1}^{n} \lambda_i(t)x_i^2$$

$$\leq \lambda_{\max}(t) \sum_{i=1}^{n} x_i^2 = \lambda_{\max}(t)\|\mathbf{x}(t)\|^2.$$

Where in $(*)$ we used that $\mathbf{x} = \sum_{i=1}^{n} x_i e_i$ with $\|e_i\| = 1$ and $e_i \perp e_j$ for all $i \neq j$. Thus we get

$$\frac{\frac{1}{2} \frac{d}{dt} \|\mathbf{x}(t)\|^2}{\|\mathbf{x}(t)\|^2} \leq \lambda_{\max}(t) \implies \int_{t_0}^{t} \log\left(\frac{\|\mathbf{x}(s)\|^2}{\|\mathbf{x}(t_0)\|^2}\right) ds \leq \lambda_{\max}(s)ds.$$

By exponentiating both sides, we obtain

$$\|\mathbf{x}(t)\| \leq \|\mathbf{x}(t_0)\| \exp\left(\int_{t_0}^{t} \lambda_{\max}(s)ds\right).$$

Therefore, by the continuation theorem, global solutions exist as long as $\int_{t_0}^{t} \lambda_{\max}(s)ds < \infty$.

2.4   Dependence on initial conditions

Given the IVP

$$\begin{cases} \dot{\mathbf{x}} = f(\mathbf{x}, t) \\ \mathbf{x}(t_0) = \mathbf{x}_0. \end{cases}$$

With $\mathbf{x} \in \mathbb{R}^n$ and $f \in C^r$ for some $r \geq 1$, we have the solution $\mathbf{x}(t; t_0, \mathbf{x}_0)$.

The dependence of the solution on initial data is of interest to us. This is due to us wanting the solution to be robust with respect to errors and uncertainties in the initial data. To address this, we have Theorem 2.5.
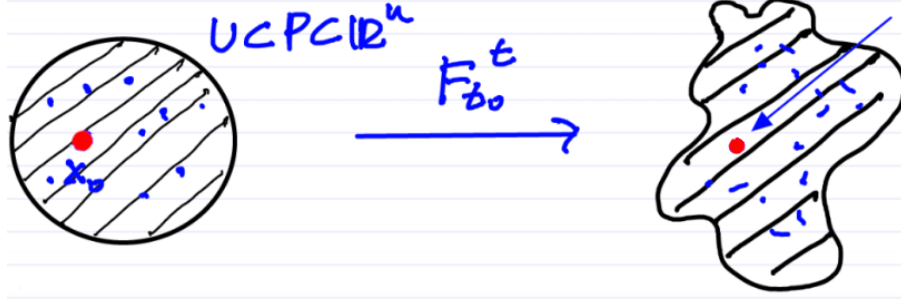
Figure 2.7: The smooth transformation of U. The red point on the right it $F_{t_0}^t(\mathbf{x}_0)$, i.e. the image of $\mathbf{x}_0$ under the evolution operator.

Theorem 2.5. *If $f \in C^r$ for $r \geq 1$ then $\boldsymbol{x}(t; t_0, \boldsymbol{x}_0)$ is C^r in $(t_0, \boldsymbol{x}_0)$. Proof in Arnold's ODE.*

The geometric meaning of this is that for $U \subset P \subset \mathbb{R}^n$ we have that $F_{t_0}^t(U)$ is a smooth deformation of U (cf. Fig. 2.7). It turns out $\left(F_{t_0}^t\right)^{-1} = F_t^{t_0}$ is also C^r, hence we have that $F_{t_0}^t$ is a diffeomorphism.

Now, how can we compute the Jacobian of the flow map $\frac{\partial \mathbf{x}(t; t_0, \mathbf{x}_0)}{\partial \mathbf{x}_0} = DF_{t_0}^t(\mathbf{x}_0)$? We start from the IVP and take the gradient (with respect to x_0) of both sides. On the left hand side we can exchange order of the time derivative and the gradient and on teh right hand side we use the chain rule. We end up with the equation

$$\frac{d}{dt} \frac{\partial \mathbf{x}}{\partial \mathbf{x}_0} = D_{\mathbf{x}} f(\mathbf{x}(t; t_0, \mathbf{x}_0), t) \frac{\partial \mathbf{x}}{\partial \mathbf{x}_0}.$$

This means, that the flow map gradient satisfies the IVP

$$\frac{d}{dt} \left[DF_{t_0}^t(\mathbf{x}_0) \right] = D_{\mathbf{x}} f(F_{t_0}^t(\mathbf{x}_0), t) DF_{t_0}^t(\mathbf{x}_0)$$
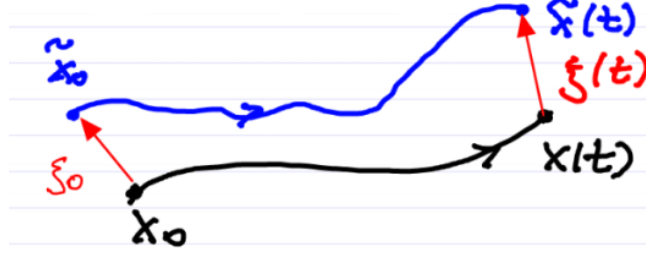
$$DF_{t_0}^{t_0}(\mathbf{x}_0) = I.$$

This is called the equation of variations, which is a linear, non-autonomous ODE for the matrix $M = DF_{t_0}^t(x_0)$

$$\begin{cases} \dot{M} = D_{\mathbf{x}} f(\mathbf{x}(t; t_0, \mathbf{x}_0)) M \\ M(t_0) = I. \end{cases}$$

Example 2.7 (Locations of extreme deformation in phase space). We define

$$\boldsymbol{\xi}(t) := \tilde{\boldsymbol{x}}(t) - \boldsymbol{x}(t) = \mathbf{x}(t; t_0, \tilde{\mathbf{x}}_0) - \mathbf{x}(t; t_0, \mathbf{x}_0)$$

$$= \mathbf{x}(t; t_0, \mathbf{x}_0) + \frac{\partial \mathbf{x}}{\partial \mathbf{x}_0}(t; t_0, \mathbf{x}_0) \boldsymbol{\xi}_0 + \mathcal{O}(\|\boldsymbol{\xi}_0\|^2) - \mathbf{x}(t; t_0, \mathbf{x}_0)$$

$$= DF_{t_0}^t(\mathbf{x}_0) \boldsymbol{\xi}_0 + \mathcal{O}(\|\boldsymbol{\xi}_0\|^2).$$

Where we used the Taylor expansion and assume the perturbation to $\mathbf{x}_0$ is small, i.e. $\|\boldsymbol{\xi}_0\| \ll 1$. Therefore we have

$$\|\boldsymbol{\xi}(t)\|^2 = \langle DF_{t_0}^t(\mathbf{x}_0)\boldsymbol{\xi}_0, DF_{t_0}^t(\mathbf{x}_0)\boldsymbol{\xi}_0\rangle + \mathcal{O}(\|\boldsymbol{\xi}_0\|^3)$$
$$= \langle \boldsymbol{\xi}_0, \underbrace{\left[DF_{t_0}^t(\mathbf{x}_0)\right]^T DF_{t_0}^t(\mathbf{x}_0)}_{=:C_{t_0}^t(\mathbf{x}_0)} \boldsymbol{\xi}_0\rangle + \mathcal{O}(\|\boldsymbol{\xi}_0\|^3).$$

$C_{t_0}^t(\mathbf{x}_0)$ is known as the Cauchy-Green strain tensor (field of $n \times n$ symmetric matrices). Therefore the largest possible deformation is

$$\max_{\mathbf{x}_0, \boldsymbol{\xi}_0} \frac{\|\boldsymbol{\xi}(t)\|^2}{\|\boldsymbol{\xi}_0\|^2} = \max_{\mathbf{x}_0, \boldsymbol{\xi}_0} \frac{\langle \boldsymbol{\xi}_0, C_{t_0}^t(\mathbf{x}_0)\boldsymbol{\xi}_0\rangle}{\|\boldsymbol{\xi}_0\|^2} = \max_{\mathbf{x}_0} \lambda_n(\mathbf{x}_0).$$

Where we used that $C_{t_0}^t$ is positive definite in the last equality, and that $\lambda_n(\mathbf{x}_0)$ is the largest eigenvalue of $C_{t_0}^t(\mathbf{x}_0)$. Because we typically have exponential growth we introduce the following quantity.

Definition 2.3. The finite-time Lyapunov exponent is defined as

$$\boxed{\mathrm{FTLE}_{t_0}^t(\mathbf{x}_0) := \frac{1}{2(t - t_0)} \log(\lambda_n(\mathbf{x}_0)).}$$

The FTLE is a diagnostic quantity for Lagrangian Coherent Structures (LCS), i.e. influential surfaces governing the evolution in P.

The ridges of $\mathrm{FTLE}_{t_0}^t$ are the repelling LCS, meanwhile the ridges of $\mathrm{FTLE}_t^{t_0}$ are the attracting LCS as depicted in Fig. 2.8. Now we are left with the problem of computing $F_{t_0}^t(\mathbf{x}_0)$. Recall that analytically we start with $F_{t_0}^t(\mathbf{x}_0)$ and use this to calculate $DF_{t_0}^t(\mathbf{x}_0)$. From here we can find $C_{t_0}^t(\mathbf{x}_0)$, giving us $\lambda_n(\mathbf{x}_0)$ and thereby the FTLE. We now outline a process to compute the FTLE numerically.

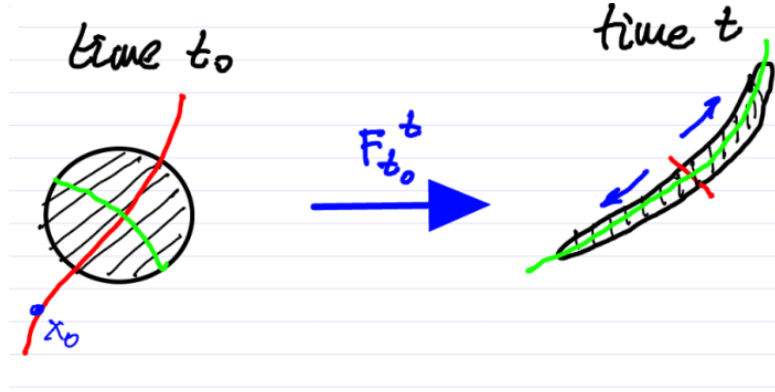(i) Define an initial $M \times N$ grid of initial data $\mathbf{x}_0(i, j) \in \mathbb{R}^2$.

Figure 2.8: On the left the red ridge represents large values of $\text{FTLE}_{t_0}^t$, on the right the green ridge the high values of $\text{FTLE}_t^{t_0}$.
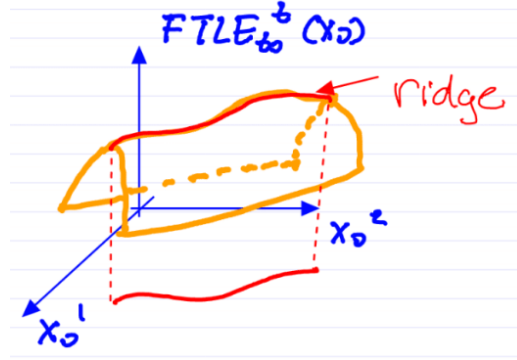

Figure 2.9: The projection of the FTLE ridge onto the initial value space.

(ii) Launch trajectories numerically from grid points to obtain a discrete approximation of $F_{t_0}^t(\mathbf{x}_0)$ as $F_{t_0}^t(\mathbf{x}_0(i,j))$.

(iii) Use finite differencing to approximate $DF_{t_0}^t(\mathbf{x}_0(i,j))$.

This process then yields the surface we see in Fig. 2.9.

Example 2.8 (Calculating the FTLE for the double gyre). Due to incompressibility, we can define the two dimensional flow using a single scalar function called the stream function.

$$\Psi(x,y) = -\sin(\pi x)\sin(\pi y).$$

The components (u,v) of the fluid velocity ($\boldsymbol{v} = (u,v)$) are obtained as partial derivatives of

the stream function, according to the formulas

$$\begin{cases} u = \dfrac{\partial \Psi}{\partial y} \\ v = -\dfrac{\partial \Psi}{\partial x}. \end{cases}$$

The Lagrangian trajectories of fluid particles obey the differential equations (i.e. we have the fluid velocity field)

$$\begin{cases} \dot{x} = u = \dfrac{\partial \Psi}{\partial y} \\ \dot{y} = v = -\dfrac{\partial \Psi}{\partial x}. \end{cases}$$

Interestingly, in this case, the phase space coincides with the physical space spanned by the coordinates (x, y).

Remark 2.6. This is an example of a Hamiltonian system, where Ψ is the Hamiltonian (usually denoted as H).

For any autonomous Hamiltonian system we have that the Hamiltonian is constant along trajectories. We can verify this as follows

$$\frac{d}{dt}\Psi(x(t), y(t)) = \frac{\partial \Psi}{\partial x}\dot{x} + \frac{\partial \Psi}{\partial y}\dot{y} = 0.$$

So we have that trajectories are level curves of $\Psi(x, y)$. We can then derive the phase portrait from the level curves of Ψ. Further, we have that $\dot{x} = \frac{\partial \Psi}{\partial y} = -\pi \sin(\pi x)\cos(\pi y)$ which yields that $\text{sign}(\dot{x}) = -\text{sign}(\sin(\pi x))\text{sign}(\cos(\pi y))$. Putting these together we can construct the contour plot with arrows. The contour plot, and FTLE approximation are shown in Fig. 2.11.

Example 2.9 (ABC flow). Let our dynamical system be defined as follows with $A, B, C \in \mathbb{R}$

$$\begin{cases} \dot{x} = A\sin(z) + C\cos(y) \\ \dot{y} = B\sin(x) + A\cos(z) \\ \dot{z} = C\sin(y) + B\cos(x). \end{cases}$$

This is an exact solution to Euler's equations. We have an autonomous velocity field. Depending on parameters it can even generate chaotic fluid trajectories. The numerical approximation of the FTLE for the ABC flow is depicted in Fig. 2.12.
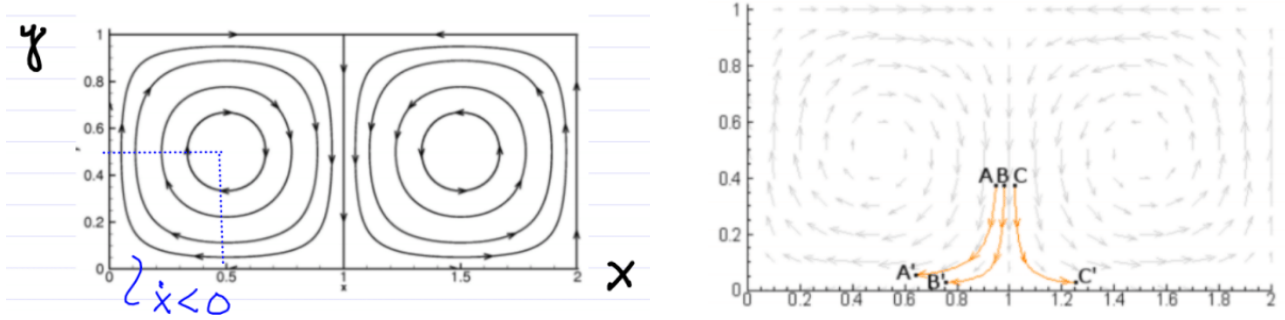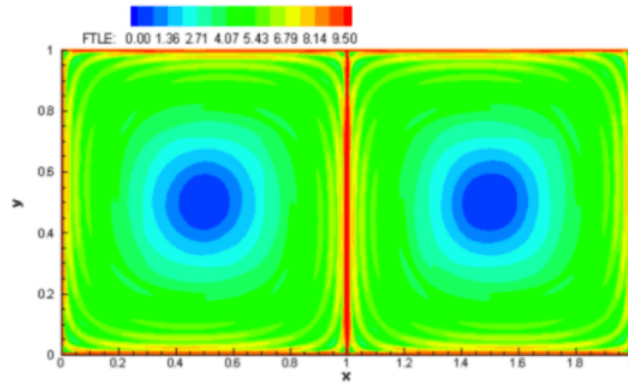
Figure 2.10:

Figure 2.11: Top left: The analytic phase plot. Top right: The exploration done to calculate FTLE. Bottom: The FTLE plot. Figures here were taken from Shawn Shadden of UC Berkeley.

2.5   Dependence on parameters

We now have the IVP

$$
\begin{cases}
\dot{\mathbf{x}} = f(\mathbf{x}, t, \boldsymbol{\mu}) \\
\mathbf{x}(t_0) = \mathbf{x}_0.
\end{cases}
$$

With $\mathbf{x} \in \mathbb{R}^n$, $f \in C^r$, $r \geq 1$, therefore we have a solution $\mathbf{x}(t; t_0, \mathbf{x}_0, \boldsymbol{\mu}) \in C^r_{\mathbf{x}_0}$.

We now examine how solutions depend $\boldsymbol{\mu}$. This is critical as solutions should be robust to changes or uncertainties in the model.

Example 2.10 (Perturbation Theory). Given a weakly nonlinear oscillator

$$
m\ddot{x} + c\dot{x} + kx = \epsilon f(x, \dot{x}, t), \ 0 \leq \epsilon \ll 1, \ x \in \mathbb{R}.
$$

The usual approach is to seek solutions by expanding from the known solution of the linear
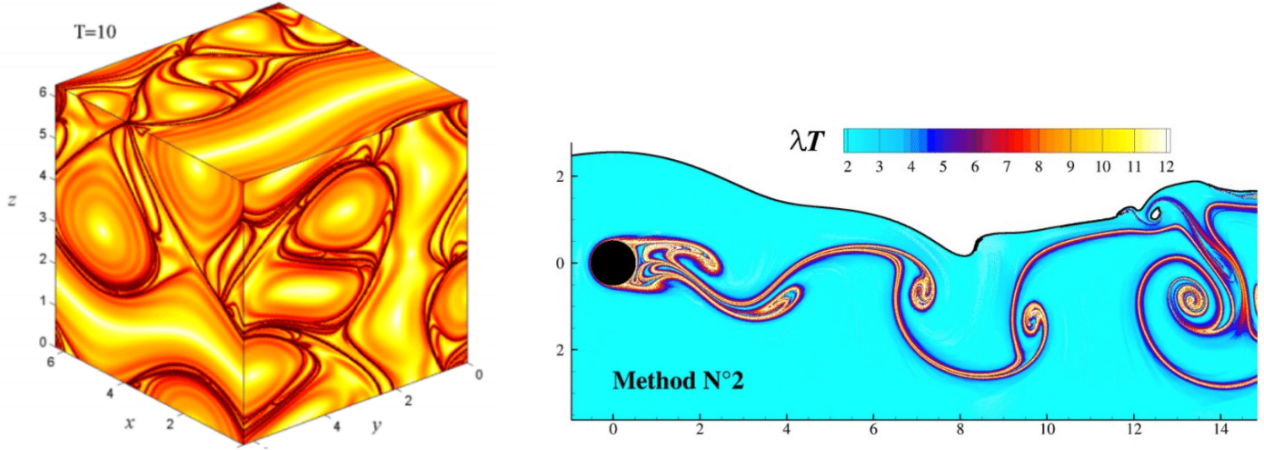
Figure 2.12: Left: numerically calculated FTLE field of the ABC flow. Darker colors signify higher FTLE values (Guckenheimer-Holmes Physica D, 2001). Right: Again the FTLE is plotted, for vortex shedding behind a cylinder under a free surface (Sun et. al, 2016).

limit $\epsilon = 0$, i.e.

$$x_\epsilon(t) = \varphi_0(t) + \epsilon\varphi_1(t) + \epsilon^2\varphi_2(t) + \ldots + \mathcal{O}(\epsilon^r).$$

If $x_\epsilon(t)$ is in C_ϵ^r, we have $\varphi_1(t) = \left.\frac{\partial x_\epsilon(t)}{\partial \epsilon}\right|_{\epsilon=0}$ and $\varphi_2(t) = \left.\frac{\partial^2 x_\epsilon(t)}{\partial \epsilon^2}\right|_{\epsilon=0}$

Regularity with respect to the parameter $\boldsymbol{\mu}$ actually follows from regularity with respect to the initial condition $\mathbf{x}_0$. We can use the following trick to extend the IVP with a dummy variable $\boldsymbol{\mu}$

$$\begin{cases} \dot{\mathbf{x}} = f(\mathbf{x}, t, u) \\ \dot{\boldsymbol{\mu}} = 0 \\ \mathbf{x}(t_0) = \mathbf{x}_0 \\ \boldsymbol{\mu}(t_0) = \boldsymbol{\mu}_0. \end{cases}$$

Thus with $\mathbf{X} = \begin{pmatrix} \mathbf{x} \\ \boldsymbol{\mu} \end{pmatrix} \in \mathbb{R}^{n+p}$ and $F(\mathbf{X}_0) = \begin{pmatrix} f \\ 0 \end{pmatrix}$; $\mathbf{X}_0 = \begin{pmatrix} \mathbf{x}_0 \\ \boldsymbol{\mu}_0 \end{pmatrix}$. We have the extended IVP

$$\begin{cases} \dot{\mathbf{X}} = F(\mathbf{X}) \\ \mathbf{X}(t_0) = \mathbf{X}_0. \end{cases} \tag{2.1}$$

Applying the previous result on regularity with respect to $\mathbf{x}_0$ to (2.1), we have that $f \in C_{\mathbf{x},\boldsymbol{\mu}}^r$ implies that $\mathbf{X}(t) \in C_{\mathbf{X}_0}^r$ in turn implying that $\mathbf{x}(t; t_0, \mathbf{x}_0, \cdot) \in C_{\boldsymbol{\mu}}^r$. The solution is as smooth in parameters as the RHS of the dynamical system.
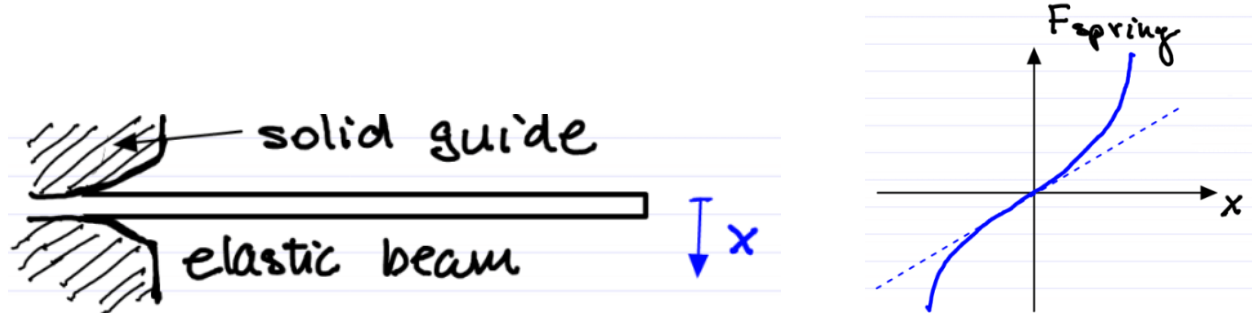
Figure 2.13: Setup for the nonlinear springboard.

Example 2.11 (Periodic Oscillations of a nonlinear springboard). Given an elastic beam extending from a solid guide, we measure the deflection of this beam with the variable x. This system is illustrated in the left panel of Fig. 2.13. By increasing x, the effective free length of the beam is shortened, thereby stiffening the spring nonlinearly. The effect of this nonlinearity on the force exerted on the spring is illustrated in the right panel of Fig. 2.13. This setup yields the following equations of motion

$$\begin{cases} \ddot{x} + x + \epsilon x^3 = 0; & 0 \le \epsilon \ll 1 \\ x(0) = a_0; & \dot{x}(0) = 0. \end{cases}$$

So we have weak nonlinearity with no known explicit solution. Although weak, this nonlinearity is still significant, as can be seen in Fig. 2.14. Rewriting this as a first order ODE ($x_1 = x$; $x_2 = \dot{x}$), and note that the RHS is $C^r_{\mathbf{x}, \boldsymbol{\mu}}$, therefore there exists a unique local solution that is also $C^r_{\boldsymbol{\mu}}$. Thus the expansion is justified

$$x_\epsilon(t) = \varphi_0(t) + \epsilon\varphi_1(t) + \ldots + \mathcal{O}(\epsilon^r). \tag{2.2}$$

We can see that for $\epsilon = 0$ we find that $\varphi_0(t) = a_0 \cos(t)$.

Now we look specifically for T-periodic solutions, as we would expect such a solution physically, therefore we have

$$\varphi_i(t) = \varphi_i(t+T).$$

The period T still has to be determined. Plugging this Ansatz to (2.2) into the IVP to get

$$\mathcal{O}(1): \quad \ddot{\varphi}_0 + \varphi_0 \qquad\qquad = 0$$

$$\mathcal{O}(\epsilon): \quad \ddot{\varphi}_1 + \underbrace{\varphi_1}_{\omega=1} \qquad\qquad = -\varphi_0^3 = -a_0^3 \cos^3(t) = -a_0^3 \left[\frac{1}{4}\cos(3t) + \frac{3}{4}\underbrace{\cos(t)}_{\text{resonance}} \right]. \tag{2.3}$$

We can see that (2.3) is a linear oscillator with a forcing coming from the zeroth order solution. Since the zeroth order solution $\varphi_0 = a_0 \cos(t)$ already solves the IVP we have the following initial conditions

$$\varphi_1(0) = 0; \quad \dot{\varphi}_1(t) = 0.$$

This holds as $\varphi_0 = a_0 \cos(t)$ already solves the IVP. The general solution to this equation is the sum of two terms. We add the general solution of the homogeneous part and a particular solution to the inhomogeneous part. We can write this solution to (2.3) as

$$\begin{aligned}
\varphi_1(t) &= \varphi_1^{\text{hom}}(t) + \varphi_1^{\text{part}}(t) \\
&= \underbrace{A\cos(t) + B\sin(t)}_{\text{TBD from initial conditions}} + \underbrace{C\cos(3t) + Dt\cos(t) + Et\sin(t)}_{\text{TBD from (2.3)}}.
\end{aligned}$$

Observe due to a resonance between the natural frequency of the oscillator and the forcing secular terms, $t\cos(t)$ and $t\sin(t)$ appear. Thus it cannot be periodic, so our Ansatz already fails for $i = 1$. We conclude that no solution of this type exists. Our Ansatz was too restrictive and T should depend on ϵ.
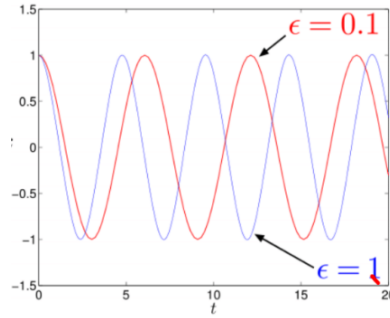

Figure 2.14: Numerical integration of x for $a_0 = 1$ and different values of ϵ.

Lindstedt's idea We should seek a solution of the form

$$x_\epsilon(t) = \varphi_0(t; \epsilon) + \epsilon\varphi_1(t; \epsilon) + \epsilon^2\varphi_2(t; \epsilon) + \mathcal{O}(\epsilon^3).$$

Furthermore φ_i should be T_ϵ periodic, i.e. the period should depend on the strength of the nonlinearity ϵ.

$$\varphi_i(t + T_\epsilon; \epsilon) = \varphi_i(t; \epsilon).$$

Rewriting the period as

$$T_\epsilon = \frac{2\pi}{\omega(\epsilon)}; \quad \omega(\epsilon) = 1 + \epsilon\omega_1 + \epsilon^2\omega_2 + \mathcal{O}(\epsilon^3).$$

We then rescale time according to $\tau = \omega(\epsilon)t$ to find

$$\frac{d}{d\tau} = \frac{1}{\omega(\epsilon)}\frac{d}{dt} \implies \boxed{[\omega(\epsilon)]^2 x'' + x + \epsilon x^3 = 0.}$$

Where we have taken x' to represent $\frac{dx}{d\tau}$. Plugging in our new Ansatz into the rescaled ODE yields

$$\left(1 + 2\epsilon\omega_1 + \mathcal{O}(\epsilon^2)\right)\left[\varphi_0'' + \epsilon\varphi'' + \mathcal{O}(\epsilon^2)\right] + \left[\varphi_0 + \epsilon\varphi_1 + \mathcal{O}(\epsilon^2)\right] + \epsilon\left[\varphi_0^3 + \mathcal{O}(\epsilon)\right] = 0.$$

Matching equal powers of ϵ yields

$$\mathcal{O}(1): \ \varphi_0'' + \varphi_0 = 0 \implies \varphi_0(\tau) = a_0\cos(\tau); \quad \varphi_0(0) = a_0; \quad \dot{\varphi}_0(0) = 0$$

$$\mathcal{O}(\epsilon): \ \varphi_1'' + \varphi_1 = -\phi_0^3 - 2\omega_1\varphi_0'' = \left(2\omega_1 a_0 - \frac{3}{4}a_0^3\right)\underbrace{\cos(\tau)}_{\text{resonance}} - \frac{a_0^3}{4}\cos(3\tau);$$

$$\varphi_1(0) = 0; \quad \dot{\varphi}_1(0) = 0.$$

From the first line, we can see the initial conditions are fulfilled. In this step we used that $\dot{\varphi}(t = 0) = 0$ if and only if $\omega(\epsilon)\varphi'(0) = 0$. We get the solution

$$\varphi_1(t) = A\cos(\tau) + B\sin(\tau) + C\cos(3\tau) + D\tau\cos(\tau) + E\tau\sin(\tau).$$

The presence of resonance again excludes periodic solutions, but now we can select ω_1 to eliminate these terms.

$$2\omega_1 a_0 - \frac{3}{4}a_0^3 = 0 \implies \boxed{\omega_1 = \frac{3}{8}a_0^2.}$$

This successfully eliminates the resonance and determines the missing frequency term at $\mathcal{O}(\epsilon)$. Thus we find

$$x_\epsilon(\tau) = a_0\cos(\tau) - \frac{\epsilon}{32}a_0^3\left(\cos(\tau) - \cos(3\tau)\right) + \mathcal{O}(\epsilon^2).$$

In the original time scaling this is

$$x_\epsilon(t) = a_0\cos(\omega t) - \frac{\epsilon}{32}a_0^3\left(\cos(\omega t) - \cos(3\omega t)\right) + \mathcal{O}(\epsilon^2); \quad \omega = 1 + \frac{3}{8}\epsilon a_0^2 + \mathcal{O}(\epsilon^2).$$

This procedure can be continued to higher order terms, where we select ω_2 so that the $\mathcal{O}(\epsilon^2)$ terms cancel.
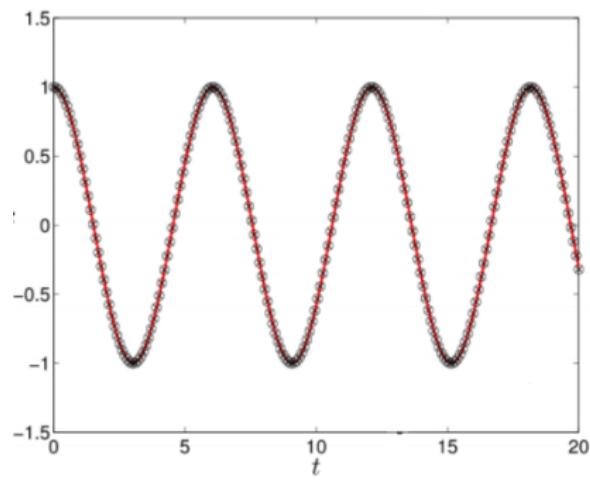
Figure 2.15: Approximation (dots) vs analytic solution (solid line) of x on the time interval $[0, 20]$.

Chapter 3

Stability of fixed points

Now we would like to begin to explore the behavious of dynamical systems around fixed points. This will allow us to find out if we should expect to observe a fixed state, and to understand what happens if we perturb the system away from this fixed state.

3.1 Basic definitions

Consider

$$\dot{\boldsymbol{x}} = f(\boldsymbol{x}, t), \ \boldsymbol{x} \in \mathbb{R}^n, \ f \in C^1.$$

Assume that $\boldsymbol{x} = 0$ is a fixed point, i.e. $f(\boldsymbol{0}, t) = \boldsymbol{0}$ for all $t \in \mathbb{R}$. If the fixed point is originally at $\boldsymbol{x}_0 \neq \boldsymbol{0}$, shift it to zero by letting $\tilde{\boldsymbol{x}} := \boldsymbol{x} - \boldsymbol{x}_0$, therefore

$$\dot{\tilde{\boldsymbol{x}}} = \dot{\boldsymbol{x}} = f(\boldsymbol{x}_0 + \tilde{\boldsymbol{x}}, t) = \tilde{f}(\tilde{\boldsymbol{x}}, t).$$

We would like to understand how the dynamical system behaves near its equilibrium state. To this end we introduce the following definitions.

Definition 3.1 (Lyapupnov Stability). $\boldsymbol{x} = \boldsymbol{0}$ is stable if for all t_0, for all $\epsilon > 0$ small enough, there exists a $\delta = \delta(t_0, \epsilon)$, such that for all $\boldsymbol{x}_0 \in \mathbb{R}^n$ with $\|\boldsymbol{x}_0\| \leq \delta$, we have

$$\|\boldsymbol{x}(t; t_0, \boldsymbol{x}_0)\| \leq \epsilon \quad \forall t \geq t_0.$$

Example 3.1 (Stability of lower equilibrium of the pendulum). Recall the equation of motion of the pendulum $\ddot{\varphi} + \sin(\varphi) = 0$, that we transform into a first order ODE by setting $x_1 = \varphi$
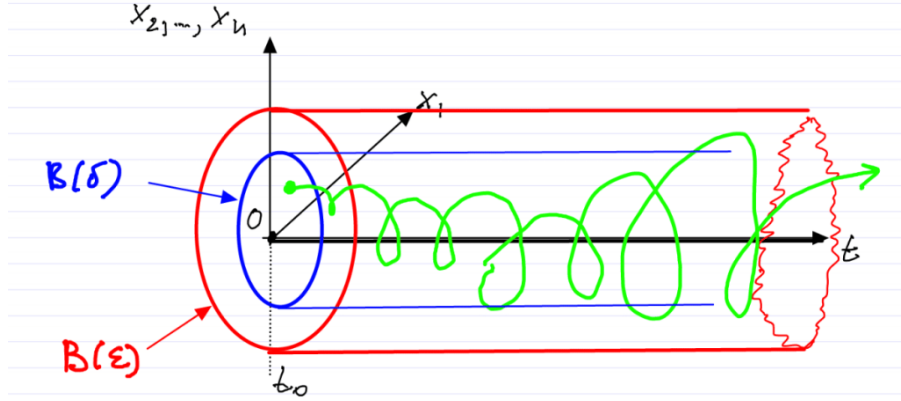
Figure 3.1: An example such a δ, $B(r)$ represents the n-dimensional ball of radius r.

and $x_2 = \dot{\varphi}$ to obtain

$$\begin{cases} \dot{x}_1 = x_2 \\ \dot{x}_2 = -\sin(x_1). \end{cases}$$

For small $\epsilon > 0$, this geometric procedure gives a $\delta(\epsilon) > 0$ such that the definition of stability is satisfied for $\boldsymbol{x} = 0$. We can see in Fig. 3.2 that for any point chosen within the blue circle, it's trajectory remains within the red circle for all time (cf. Fig. 3.1. Therefore $\boldsymbol{x} = 0$ is (Lyapunov) stable.
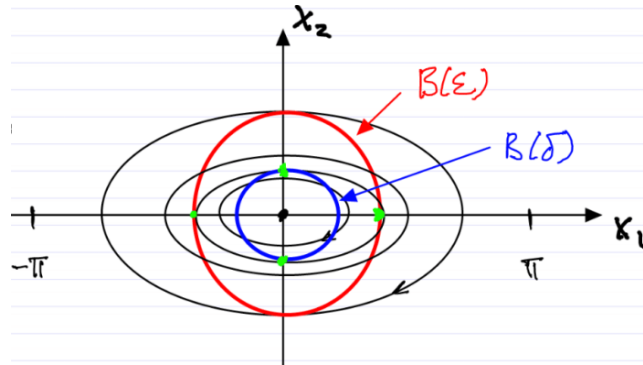

Figure 3.2: Stability of lower equilibrium for the pendulum, here $0 < \epsilon < \pi$.

Definition 3.2 (Asymptotic stability)**.** The fixed point $\boldsymbol{x} = 0$ is *asymptotically stable* if

   (i) it is stable,

(ii) for all t_0, there exists $\delta_0(t_0)$ such that for every $\boldsymbol{x}_0$ with $\|\boldsymbol{x}_0\| \leq \delta_0$ we have

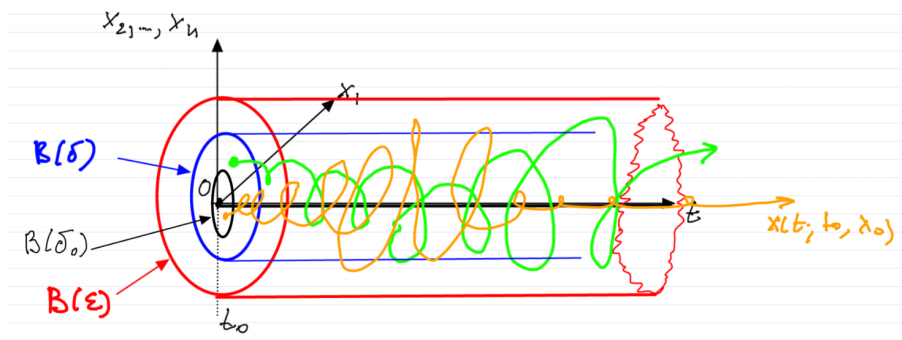$$\lim_{t \to \infty} \boldsymbol{x}(t; t_0, \boldsymbol{x}_0) = 0.$$

Figure 3.3: An example for an asymptotically stable fixed point (black trajectory).

Definition 3.3 (Domain of attraction). The *domain of attraction* is the set of all $\boldsymbol{x}_0$'s for which

$$\lim_{t \to \infty} \boldsymbol{x}(t; t_0, \boldsymbol{x}_0) = 0.$$

Example 3.2 (Damped pendulum). We have the equation of motion with the linear damping coefficient c

$$\ddot{\varphi} + c\dot{\varphi} + \sin(\varphi) = 0, \quad c > 0.$$

Transforming into a first-order ODE with $x_1 = \varphi$ and $x_2 = \dot{\varphi}$ gives
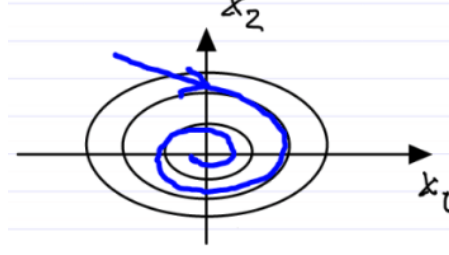
$$\begin{cases} \dot{x}_1 = x_2 \\ \dot{x}_2 = -cx_2 - \sin(x_1). \end{cases}$$

The total energy is given by

$$E = \frac{1}{2}x_2^2 + (1 - \cos(x_1)).$$

Further we have the rate of energy change

$$\frac{d}{dt}E(x_1(t), x_2(t)) = x_2\left(\dot{x}_2 + \sin(x_1)\right) = -cx_2^2.$$

Therefore, along trajectories energy decreases monotonically. By the C^0 dependence of the trajectory on initial conditions, the trajectories remain close to the undamped oscillations for small $c > 0$. We conclude that trajectories are inward spirals for a small dissapation $c > 0$ small. The fixed point $\boldsymbol{x} = 0$ is still Lyapunov stable, but asymptotic stability does not yet follow (is the limit of $\boldsymbol{x}(t)$ equal to 0?).

Remark 3.1 (LaSalle's invariance principle). This conclusion follows rigorously from LaSalle's invariance principle, namely if we assume that $\dot{\boldsymbol{x}} = f(\boldsymbol{x})$, $f \in C^1$, and that there exists a $V \in C^1$ with

$$\dot{V} = \frac{dV(\boldsymbol{x}(t))}{dt} \leq 0.$$

Then the set of accumulation points for any trajectory is contained in the set of trajectories that stay within the set $I = \{\boldsymbol{x} \in \mathbb{R}^n : \dot{V}(\boldsymbol{x}) = 0\}$.

Example 3.3. Consider the following dynamical system in polar coordinates, i.e. $r\cos(\theta) = x$ and $r\sin(\theta) = y$,

$$\begin{cases} \dot{r} = r(1 - r) \\ \dot{\theta} = \sin^2\left(\dfrac{\theta}{2}\right). \end{cases}$$

Note that $r = 0$ is a fixed point, the set $r = 1$ is an invariant circle, and the set $\theta = 0$ is an invariant set. An invariant set is a set such that if the dynamical system is started on the set, it remains in the set for all time. Examining the radial evolution reveals that the equation of motion decouples. We see that $\dot{\theta} \geq 0$, so rotation is either positive or null.

However, we have that $p = (1, 0)$ is an example of an attractor: a set with an open neighborhood of points that all approach the set as $t \to \infty$.

Definition 3.4 (Invariant set). The set $S \subset P$ is an *invariant set* for the flow map $F^t : P \to P$ if $F^t(S) = S$ for all $t \in \mathbb{R}$.

Definition 3.5 (Unstable point). A fixed point $\boldsymbol{x} = 0$ is unstable if it is not stable.
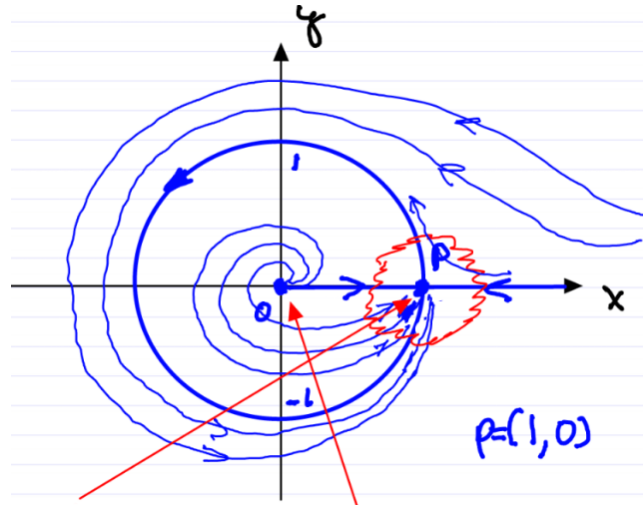
Figure 3.4: Phase portrait of the dynamical system, with the red arrows pointing to the two unstable equilibria.

Remark 3.2. We can negate a mathematical statement by using the reverse relational operators outside the statements involving these operators i.e. $\exists \to \forall$ and $\forall \to \exists$. For example we have for continuity $\forall \epsilon \, \exists \delta : \, \|f(\boldsymbol{x}) - f(\boldsymbol{y})\| < \epsilon$ if $\|\boldsymbol{x} - \boldsymbol{y}\| < \delta$, meanwhile for discontinuity we have $\exists \epsilon : \, \forall \delta : \, \|f(\boldsymbol{x}) - f(\boldsymbol{y})\| \geq \epsilon$ for $\|\boldsymbol{x} - \boldsymbol{y}\| < \delta$.

In our case for stability we have

$$\forall \epsilon, t_0 : \quad \exists \delta > 0 : \quad \forall \boldsymbol{x}_0 \text{ with } \|\boldsymbol{x}_0\| < \delta : \quad \|\boldsymbol{x}(t)\| \leq \epsilon \quad \forall t \geq t_0.$$

Meanwhile for instability

$$\exists \epsilon, t_0 : \quad \underbrace{\forall \delta > 0}_{\text{“for arbitrarily small”}} \quad : \quad \exists \boldsymbol{x}_0 \text{ with } \|\boldsymbol{x}_0\| < \delta : \quad \|\boldsymbol{x}(t)\| > \epsilon \quad \underbrace{\exists t \geq t_0}_{\text{“for some”}} .$$

This negation is demonstration in Fig. 3.5

Remark 3.3. By C^0 dependence of trajectories on initial conditions, if $\boldsymbol{x}(t; t_0, \boldsymbol{x}_0)$ leaves $B(\epsilon)$, then for $\tilde{\boldsymbol{x}}_0$ close enough to $\boldsymbol{x}_0$, $\boldsymbol{x}(t; t_0, \tilde{\boldsymbol{x}}_0)$ also leaves $B(\epsilon)$. Since this is true on an open set around $\boldsymbol{x}_0$, the measure of such trajectories in nonzero, the instability is observable!

Example 3.4 (Unstable fixed point of pendulum). In constrast, we can have that infinitely many trajectories converge to the fixed point, yet it is still unstable. In fact, the converging trajectories form a measure-zero set, thus the stability near the unstable equilibrium is unobservable.
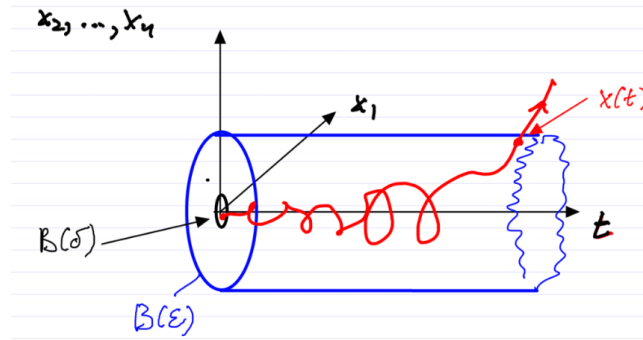
Figure 3.5: Example of an unstable fixed point, with the red trajectory representing a trajectory starting arbitraritly close to the fixed point, leaving a given ϵ-ball.
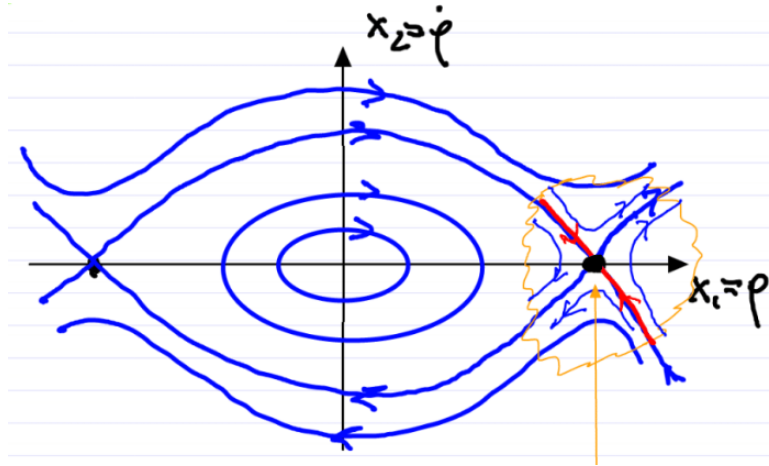

Figure 3.6: The phase portrait around the unstable fixed point of the pendulum, with the stable trajectories (red).

3.2   Stability based on linearization

We would like to derive a more general method to analyze the stability of fixed points, thus we try to simplify our system around the fixed point and discover what this can tell us about the full (unsimplified) system. In the following section we shall always assume that our system is autonomous. We will have the following setup

$$\dot{\boldsymbol{x}} = f(\boldsymbol{x}), \quad f \in C^1, \quad \boldsymbol{x} = \begin{pmatrix} x_1 \\ \vdots \\ x_n \end{pmatrix} \in \mathbb{R}^n, \quad \boldsymbol{p} = \begin{pmatrix} p_1 \\ \vdots \\ p_n \end{pmatrix} \in \mathbb{R}^n.$$